Applied Catalysis B: Environmental 140–141 (2013) 506–515

Contents lists available at SciVerse ScienceDirect

Applied Catalysis B: Environmental

journal homepage: www.elsevier.com/locate/apcatb

Cu-containing MFI zeolites as catalysts for wet peroxide oxidation of formic acid as model organic contaminant

Oxana P. Taran[a,b,*], Svetlana A. Yashnik[a], Artemiy B. Ayusheev[a], Anna S. Piskun[a], Roman V. Prihod'ko[c], Zinfer R. Ismagilov[a], Vladislav V. Goncharuk[c], Valentin N. Parmon[a,d]

[a] Boreskov Institute of Catalysis, Siberian Branch of the Russian Academy of Sciences, 5 prosp. Lavrentieva, Novosibirsk 630090, Russia
[b] Novosibirsk State Technical University, 20, prosp. K. Marx, Novosibirsk 630092, Russia
[c] Dumansky Institute of Colloid and Water Chemistry, National Academy of Sciences of Ukraine, 42 blv. Vernadskogo, Kiev-142 03680, Ukraine
[d] Novosibirsk State University, 2 st. Pirogova, Novosibirsk 630090, Russia

ARTICLE INFO

Article history:
Received 21 December 2012
Received in revised form 16 April 2013
Accepted 23 April 2013
Available online 4 May 2013

Keywords:
Cu-exchanged zeolites
Cu-ZSM-5
Catalytic wet peroxide oxidation
Formic acid

ABSTRACT

The catalytic behavior of different Cu(Fe)/zeolite catalysts with the MFI morphology in wet peroxide oxidation of formic acid as a model organic substrate was thoroughly examined. The influence of the method for Cu^{2+} ions introduction into the zeolite matrix, Cu loading and the electron state of Cu on catalytic properties of zeolites, including their stability to leaching of Cu was studied. Cu-substituted ZSM-5 zeolites with the atomic ratio Si/Al = 30 and Cu content of 0.5–1.5, which were prepared by ion exchange, were shown most promising for wet peroxide oxidation. The impact of temperature, initial pH and concentrations of reagents on the catalytic performance of the catalyst with the optimal composition also was studied. The characterization of fresh and spent catalysts using UV–vis DR and ESR spectroscopic techniques led to suppose that the high efficiency of Cu-ZSM-5 to redox reactions in aqueous media is provided by nanostructured square-planar copper oxide clusters localized in the zeolite channels.

1. Introduction

Catalytic wet peroxide oxidation (CWPO) is an ecologically attractive catalytic approach aimed at deep oxidation of weakly biodegradable toxic organics in wastewater [1]. The deep oxidation of these compounds in aqueous media allows their direct removal or transformation into non-toxic products to be eliminated by biological treatment. CWPO is an efficient process for destruction of stable organic compounds under rather mild conditions (0.1–0.5 MPa, $T \leq 100\,^{\circ}C$) owing to the strong oxidizing properties of hydrogen peroxide [2]. The system comprising homogeneous iron ions and hydrogen peroxide, the so-called Fenton reagent, is an efficient oxidant of various organic substances in aqueous media [3]. Some other transition metal ions (e.g. Cu, Mn), the components of the so-called Fenton-like systems, also are active to CWPO. These systems are most appropriate for water purification from the organic compounds at their concentration lower than 10^{-2} to 10^{-3} M [4,5].

However, in spite of their efficiency in the oxidation of various organics, homogeneous catalytic systems comprising soluble transition metal ions have well-known drawbacks, e.g. a limited pH range of the operation, the formation of metal-containing sludges which are difficult to dispose, and the catalyst deactivation by some metal complexing agents. That is why the development of heterogeneous Fenton-type catalysts that cause no disposal problem and have a similar activity is of paramount interest for wastewater treatment.

Many different materials containing iron or copper supported on oxides [6–8], clays [9–11], perovskite-type oxides [12] and polymers [13] have been suggested as catalysts for the oxidation of organic compounds, but only few of them showed a significant activity and stability in aqueous media [6,10,12]. Since 1995, some interesting data have been reported regarding metal ions (Fe, Cu) containing zeolite-based catalysts as promising solid-phase catalysts for oxidation of a variety of organic pollutants in water with hydrogen peroxide, e.g. phenol and phenol derivatives [14,15], carboxylic acids [4] and some textile dyes [2,16,17]. Most of these studies dealt with the Fe-containing zeolites with the ZSM-5 (MFI) structure [4,17–19], which showed a higher catalytic activity in a wider pH range as compared to the homogeneous Fenton-like oxidation. The stability and the heterogeneous nature of the zeolite catalysts were proved in numerous consecutive catalytic

* Corresponding author at: Boreskov Institute of Catalysis, Siberian Branch of the Russian Academy of Sciences, 5 prosp. Lavrentieva, Novosibirsk 630090, Russia. Fax: +7 383 3343056.
E-mail addresses: oxanap@catalysis.ru, oxanap@bk.ru (O.P. Taran).

0926-3373/$ – see front matter © 2013 Elsevier B.V. All rights reserved.
http://dx.doi.org/10.1016/j.apcatb.2013.04.050

experiments showing negligible contribution of homogeneous catalysis of leached iron ions. There are only few data on catalytic properties of Cu-containing zeolites available in literature [20,21]. However the copper containing catalysts such as Al–Cu catalyst supported on pillared clay and CuO catalyst supported on Al_2O_3 were reported very active to oxidation of phenol dissolved in water [22]. The CuFe-ZSM-5 catalyst demonstrated even higher activity than Fe-ZSM-5 [17,23].

Here, we report our systematic study of CWPO of formic acid over Cu–zeolite catalysts with the MFI structure. The aim was to develop an active and stable Cu–zeolite catalyst based on certain knowledge of the structure of the active catalytic center and few principal features of the reaction mechanism.

The studies were focused on the influence of the Cu electron state on catalytic properties of zeolites, including their stability to leaching of Cu. The electron state of copper ions in the fresh and spent catalysts was studied by UV–vis- and ESR-spectroscopy. The impact of the reaction conditions on the catalytic performance at the optimal catalyst composition also was studied.

Formic acid, an intermediate in deep oxidation of most organic compounds [24] and the main reason for leaching of active components of the catalysts into the reaction solution, was chosen as the model organic substrate. Oxidation of formic acid does not produce a variety of intermediates like those formed, e.g. in the course of phenol oxidation. In this case the analysis of the results is much simpler than with more complex substrates. Moreover our early studies [25] showed that the regularities of the peroxide oxidation of phenol, ethanol, and formic acid are similar in many respects.

2. Experimental

2.1. Chemicals

The following reagents were used without additional purification: HCOOH (98%, PA-ACS, Panreac), CH_3COOH (chemical purity grade, Reakhim), H_2O_2 (special purity grade, Reakhim), $TiCl_4$ (special purity grade, Kristall Co.), H_2SO_4 (special purity grade, Reaktiv), C_2H_5OH (for chromatography, Reakhim), KH_2PO_4 (special purity grade, Reakhim), CH_3CN (special purity grade, Kriokhrom). Milli-Q water (Millipore, France) was used for preparing all the solutions.

2.2. Catalyst preparation

Cu-ZSM-5 catalysts were synthesized using commercial samples (Novosibirsk Chemical Concentrates Plant, Russia) of H-ZSM-5 zeolites with different Si/Al ratios (zeolite module). The H-ZSM-5 zeolite samples were characterized earlier [26]. These are well-crystallized zeolites with the crystallinity degree not less than 95%. ^{27}Al NMR data indicated the absence of extra-lattice Al^{3+} ions in the samples except the sample with the module equal to 17 where the content of these ions was ca. 10%. The chemical composition given by X-ray fluorescent analysis and textural characteristics of the zeolite samples are shown in Table 1.

Cu-ZSM-5 and Fe-ZSM-5 catalysts (see Table 2) were prepared by ion exchange between H-ZSM-5 zeolite [26] and aqueous solution of copper acetate (pH 6) or iron chloride and iron oxalate during 48 h at room temperature. The copper salt concentration varied from 0.06 to 0.125 M at the solution to zeolite weight ratio equal to 10. H-ZSM-5-17 zeolite (0.09 wt% Fe as framework iron) was used for preparation of Fe-ZSM-5 catalysts. A total of iron content in the samples was 0.16 wt% and 1.59 wt% (Table 2, Nos. 2 and 3, respectively). The suspension was filtered, the precipitate washed with distilled water until copper or iron ions were not detected in the filtrate. The Cu- and Fe-containing samples were dried in air at 343–353 K for 2 h and calcined in air at 773 K for 4 h. The samples were designated as α%Cu(Fe)-ZSM-5-β, where α is copper or iron content, β is Si/Al atomic ratio.

Cu-containing silicate catalysts with the MFI structure were synthesized by the method of solid-phase transformation (SST) under hydrothermal conditions [27]. An aqueous solution of tetrapropylammonium hydroxide (TPAOH, 7 ml, 26 wt%) was added to 1 g of kanemite powder ($NaHSi_2O_5{\cdot}3H_2O$) under stirring. Then, 3 ml of the solution containing the required quantity of $Cu(NO_3)_2{\cdot}3H_2O$ (19.25, 38.50, 77.00 mg) was added and the suspension was heated up to 343 K and kept for 3 h under vigorous stirring. The mixture was cooled to room temperature; nitric acid was added to decrease pH down from 13.0 to 8.5. The solid precipitate was washed with distilled water, filtered out and dried at 298 K for 18 h. The resulting powder was put into a 5 ml glass ampoule, sealed and then heated at 403 K for 72 h. The samples obtained were calcined at 773 K in flowing air for 20 h.

2.3. Characterization of the catalysts

The contents of copper, iron and aluminum in Cu-ZSM-5 and Fe-ZSM-5 samples (before and after their testing in CWPO) and in the filtrates after the reaction were detected by ICP-AES with a spectrophotometer Optima 4300 DV (Perkin-Elmer Inc., USA).

Structures of copper-containing silicates were studied by XRD with a HZG-4C diffractrometer (Fre/Berger Prazisionmechanik) with monochromatic CuK_α radiation (λ = 1.54178 Å).

Diffuse reflection electron spectroscopy (UV–vis DR) and electron spin resonance (ESR) were used for studying copper electron states in the Cu-containing catalysts. UV–vis DR spectra were acquired using a spectrophotometer Shimadzu UV-2501PC equipped with a diffuse reflection unit ISR-240A. $BaSO_4$ was used as a reference. The spectra were presented in the form of the Kubelka–Munk function, F(R). ESR spectra of the samples were acquired using a Bruker ER 200D spectrometer with microwave region λ = 3 cm, a 100 kHz high-frequency modulation of magnetic field and magnetic field up to 5000 G at 77 and 300 K in a quartz glass ampoule with the internal diameter of 3 mm. Parameters of the ESR spectra were determined by comparing them with the spectrum of a diphenylpicrylhydrazyl (DPPH, $g = 2.0037 \pm 0.0002$).

2.4. Catalytic testing

The formic acid oxidative destruction was carried out in a thermostated three-necked glass slurry reactor at 303 K under continuous stirring (900 rpm) with a magnetic stirrer. Typical concentrations of formic acid and hydrogen peroxide were 0.1 and 1 mol L^{-1}, respectively. The volume of solution was 110 ml. The typical initial pH was equal to 2.3, pH being not corrected during the reaction. The quantity of hydrogen peroxide was taken as large as

Table 1
Chemical composition and textural properties of initial H-ZSM-5 samples.

No.	Sample	Chemical composition (wt%)							Si/Al (atom)	S_{BET} ($m^2\,g^{-1}$)	S_{extern} ($m^2\,g^{-1}$)	V_{sum} ($cm^3\,g^{-1}$)	V_{micro} ($cm^3\,g^{-1}$)
		Al	Si	K	Na	Mg	Ca	Fe					
1	H-ZSM-5-17	2.16	39.6	0.02	0.05	0.02	0.04	0.09	17	385	104	0.200	0.122
2	H-ZSM-5-30	1.43	42.89	0.01	0.06	0.03	0.04	0.65	30	450	166	0.255	0.125
3	H-ZSM-5-45	0.97	43.35	0.01	0.00	0.03	0.06	0.60	45	346	127	0.239	0.095

Table 2
Catalytic activity of zeolites in formic acid oxidation by hydrogen peroxide (0.1 M HCOOH, 1 M H_2O_2, 3 g L^{-1} catalyst, pH_0 2.3, 303 K).

No.	Type of zeolite	Content			W (mmol L^{-1} min^{-1})[a]	A (mmol min^{-1} $g_{kat}{}^{-1}$)[b]	CA (mmol min^{-1} $g_{Me}{}^{-1}$)[c]	TOC, conversion (%)[d]
		Si/Al	Fe (wt%)	Cu (wt%)				
1	ZSM-5	17	0.09	–	0.16	0.032	36	98.5
2			0.16	–	0.23	0.046	29	84.8
3			1.59	–	0.17	0.034	2.1	97.6
4			0.09	0.3	0.62	0.21	70	99.2
5			0.09	0.48	0.69	0.23	48	99.7
6			0.09	0.76	0.78	0.24	32	99.4
7			0.09	0.95	0.91	0.26	27	99.8
8			0.09	1.35	0.93	0.31	23	99.7
9[e]			0.09	2.0	0.77	0.25	12.5	99.1
10		30	0.65	–	0.69	0.15	23	99.2
11			0.65	0.05	0.73	0.24	480	99.1
12			0.65	0.1	0.99	0.33	330	99.3
13			0.65	0.2	1.3	0.45	225	99.7
14[e]			0.65	0.3	0.99	0.33	110	99.1
15			0.65	0.5	1.0	0.34	68	99.7
16			0.65	0.7	1.3	0.44	63	99.6
17			0.65	0.9	1.2	0.39	43	99.8
18[e]			0.65	1.5	1.5	0.50	33	99.6
19[e]			0.65	2.8	1.4	0.45	16	99.7
20		45	0.6	–	0.51	0.11	19	98.9
21			0.6	0.3	0.97	0.32	107	99.7
22			0.6	0.6	0.97	0.32	53	99.5
23			0.6	0.9	1.1	0.38	42	99.1
24			0.6	1.2	1.0	0.35	29	99.6
25			0.6	2.3	1.1	0.39	17	99.6
26[e]	SST	–	–	0.5	0.023	0.0078	1.6	93.3
27[e]		–	–	1.0	0.057	0.019	1.9	95.5

[a] Rate of substrate decrement calculated from the linear fragment of kinetic curve.
[b] Catalytic activity per gram of catalyst.
[c] Catalytic activity per gram of Cu or Fe for copper- and iron-containing catalysts, respectively.
[d] TOC content was determined upon complete destruction of formic acid except the cases of a very low catalyst activity that made it unreasonable to conduct the reaction till the complete destruction.
[e] After the reaction, the filtrates were used for studying catalytic activity of homogeneous copper ions.

10 times of the oxidative equivalents for oxidation of formic acid to carbon dioxide and water. An approximately constant (±10% of the initial concentration) H_2O_2 concentration was maintained all along the reaction. The reaction started upon addition of a catalyst sample (3 g L^{-1}, 330 mg). At regular time intervals, aliquots (1 ml) were taken from the reactor to monitor the substrate and H_2O_2 concentrations. Samples were stabilized by adding ethanol at the ratio 1:1. In this work, each experiment was repeated 3 times to assess the reproducibility of the results.

A total of organic carbon (TOC) content was determined upon complete destruction of formic acid except the cases of a very low catalyst activity that made it unreasonable to expect completing of the reaction.

The catalyst stability to leaching the active component was estimated based on the ICP-AES measurement of quantity of leached copper, iron and aluminum in the reaction solution.

The contribution of dissolved copper ions (homogeneous component) to the catalytic activity was identified as follows. After the reaction in the presence of a solid catalyst was finished, the catalyst suspension was filtered out using acetatecellulose membrane filters (pore diameter 0.20 μm). The filtrate was placed in a thermostated reactor, the substrate and hydrogen peroxide were added in the necessary quantities. The reaction was conducted under conditions identical to the heterogeneous catalytic reaction.

Repeated testing aimed at checking the stability of the catalytic performance was achieved as follows. After the end of a cycle of the catalyst testing, the catalyst was separated by centrifuging, washed with distilled water, dried in air at 423 K, and weighed. The dry catalyst was used for the next oxidation cycle.

The influence of pH on the oxidation kinetics was studied with the 1.5%Cu-ZSM-5-30 catalyst over the pH range between 2.3 and 6.5. A NaOH solution was added to the formic acid solution to obtain required pH and was not corrected during the reaction.

The influence of the substrate and oxidant concentrations on the reaction kinetics was studied experimentally by varying the initial substrate concentration in the range of 0.1–1 M at a constant inlet concentration of hydrogen peroxide (maintained at 1 M) or by varying the oxidant concentration (0.1–2 M) at a constant concentration of formic acid (0.1 M). The oxidant concentration was maintained at a required constant level during the reaction. *Different weighed samples* (0.38–6 g L^{-1}) were used at identical initial concentrations of formic acid (0.1 M) and hydrogen peroxide (1 M) for determining the reaction order in respect of the catalyst.

Conversions of formic acid (X_{FA}) and total organic carbon (X_{TOC}) were calculated by formulae:

$$X_{FA}(\%) = \frac{C^0_{FA} - C_{FA}}{C^0_{FA}} \times 100; \qquad X_{TOC}(\%) = \frac{C^0_{TOC} - C_{TOC}}{C^0_{TOC}} \times 100;$$

where C^0 is the initial concentration of the substrate in the solution, C is the current substrate concentration.

Catalytic properties of zeolite samples were compared using a catalytic activity (A, mmol min^{-1} $g_{cat}{}^{-1}$) and a specific catalytic activity (CA, mmol min^{-1} $g_{Me}{}^{-1}$) calculated as the reaction rate per gram of catalyst and gram of active component, respectively. The reaction rate (W, mmol L^{-1} min^{-1}) was calculated using the kinetic curve. The typical curves are S-shaped with two regions. The reaction rate increases in first region and has zero order in respect of

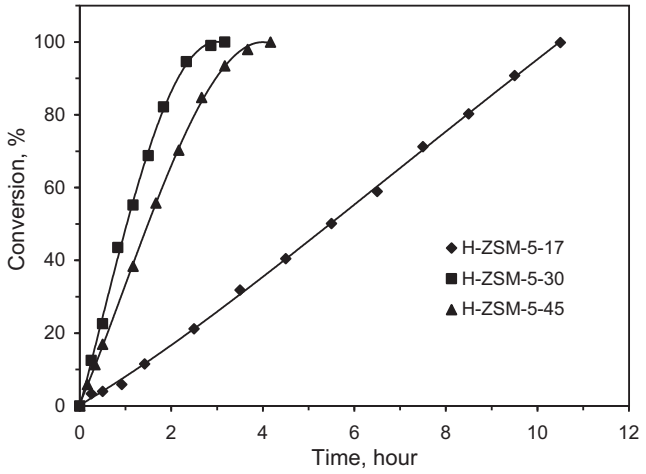

Fig. 1. Formic acid oxidation by hydrogen peroxide over H-ZSM-5 zeolites with different Si/Al ratio (0.1 M HCOOH, 1 M H_2O_2, 3 g L^{-1} catalyst, initial pH 2.3, 303 K).

the substrate concentration in the second (Fig. 2). The latter linear region was used for the calculations.

2.5. Analytic methods

A spectrophotometric method, based on the absorption of a titanium complex (λ = 410 nm) was used for determining the concentration of H_2O_2 in the solution [28]. The concentration of formic acid in the reaction solutions was measured by HPLC using a Shimadzu LC-20A with a diode array detector and Phemomenex Synergi 4u Hydro-RP 80A column (250 mm × 4.6 mm, 4 μm). Analytic conditions: eluent 0.02 M K_2HPO_4 (pH 2.90), flow rate 0.7 ml min^{-1}, column temperature 303 K. 0.1 M acetic acid was used as the internal standard. Total organic carbon (TOC content) was determined in filtered aliquots using a Shimadzu TOC Analyzer, TOC-VCSH (Japan).

3. Results and discussion

3.1. Catalytic properties of zeolites to peroxide oxidation of formic acid

Non-modified H-ZSM-5 zeolites and ion-exchanged Fe-ZSM-5 and Cu-ZSM-5 samples with different Si/Al ratios and active component contents, as well as Cu-containing silicates with the MFI type structures were tested in the reaction of formic acid oxidation (Table 2).

3.1.1. H-ZSM-5 zeolites

The iron contents in the commercial H-ZSM-5-17, H-ZSM-5-30 and H-ZSM-5-45 zeolite samples were 0.09, 0.65 and 0.6 wt%, respectively. The contribution of iron cation impurities to the catalytic activity of the Fe- and Cu-containing catalysts based on these zeolites was estimated by studying the catalytic behavior of the initial zeolites. Fig. 1 shows time dependencies of the conversion of formic acid in the presence of these zeolites. In H-ZSM-5-17 and H-ZSM-5-30 zeolites, Fe^{3+} cations are predominantly stabilized as individual ions in tetrahedral positions of the zeolite lattice ($Fe^{3+}{}_{Td}$) [26]. These cations were shown to be most stable and active to peroxide oxidation [20,32,33]. In H-ZSM-5-45 zeolite, iron cations are mainly stabilized in the form of nanodisperse extra-lattice iron(III) oxide clusters with octahedral oxygen environment ($Fe^{3+}{}_{Oh}$) [26]. Fig. 1 leads us to conclude about noticeable difference in catalytic behavior of H-ZSM-5-30 and H-ZSM-5-45 even though they comprise iron in comparable proportions but in different electron states. H-ZSM-5-30 zeolite with framework Fe^{3+} ions is a more active catalyst than H-ZSM-5-45 with extra-lattice $Fe^{3+}{}_{Oh}$ ions, its specific catalytic activity (per gram of Fe) is ca. 1.2 times higher (Table 2, Nos. 10 and 20). Compared to H-ZSM-5-30, H-ZSM-5-17 (the minimal impurity iron in the form of $Fe^{3+}{}_{Td}$) provided the rate of the substrate oxidation lower by factor of ca. 4.5 (Table 2, No. 1), but its specific catalytic activity (36 mmol min^{-1} $g_{Fe}{}^{-1}$) was somewhat higher than that of H-ZSM-5-30 (23 mmol min^{-1} $g_{Fe}{}^{-1}$). These observations may be accounted for by the fact that H-ZSM-5-17 comprise all iron cations stabilized in tetrahedral positions in the zeolite lattice while H-ZSM-5-30 some portion of extra-lattice iron cations $Fe^{3+}{}_{Oh}$.

3.1.2. Catalytic properties of Fe-ZSM-5

In order to check if the framework rather than extra-lattice Fe^{3+} ions are active to oxidation of formic acid with hydrogen peroxide, iron-substituted zeolites were studied (Table 2, Nos. 1–3). From UV–vis DR data, the incorporated Fe^{3+} ions are isolate Fe^{3+} in octahedral environment of oxygen-containing ligands which are stabilized in the ion-exchange positions (0.16%Fe-ZSM-5-17) and in oxide clusters with the structure close to α-Fe_2O_3 (1.59%Fe-ZSM-5-17). Comparative studies of the substituted Fe-ZSM-5-17 and non-modified H-ZSM-5-17 (0.09%Fe) samples did not reveal a considerable increase in the catalytic activity of the substituted zeolite (0.032, 0.046 and 0.034 mmol min^{-1} $g_{cat}{}^{-1}$ for the samples containing 0.09, 0.16 and 1.59% of Fe, respectively), while the specific catalytic activity per gram of iron was even decreased: from 36 for H-ZSM-5 to 29 and 2.1 mmol min^{-1} $g_{Fe}{}^{-1}$ after addition of 0.16% and 1.59 wt% of Fe, respectively. Hence, isolated $Fe^{3+}{}_{Oh}$ ions, both in cation positions of the zeolite and in the iron oxide clusters, are less active than the isolated ions in tetrahedral positions of the zeolite matrix ($Fe^{3+}{}_{Td}$). The observed decrease in the activity upon an increase in the percentage of the extra-lattice ions may be accounted for by blocking the zeolite channels with iron oxide nanoclusters.

Hence, the results obtained are in good agreement with literature data on the catalytic behavior of Fe-ZSM-5 zeolites with iron in different electron states [29,30].

3.1.3. Catalytic properties of Cu-ZSM-5

Cation-substituted H-ZSM-5-17 zeolite with Cu^{2+} cations rather than Fe^{3+} results in a more considerable increase in the catalytic activity (Table 2, Nos. 4–9). The catalytic activities of 0.16%Fe-ZSM-5-17 and 0.1%Cu-ZSM-5-17 were 0.032 and 0.210 mmol min^{-1} $g_{cat}{}^{-1}$, at the close contents of the modifier (0.07 and 0.10 wt% of Fe and Cu, respectively) and 0.09 wt% of the framework iron ($Fe^{3+}{}_{Td}$).

Emphasize that the S-shape is characteristic of kinetic curves of the formic acid consumption over fresh Cu-ZSM-5 catalysts, there being observed a noticeable induction period in the beginning of the reaction and then the region of zero-order kinetics in respect of the substrate. However, the induction period is not observed with the re-used catalysts. The TOC conversion measured after reaching the complete conversion of formic acid is as high as 98–99% over all zeolites under study.

Fig. 2 illustrates experimental data on the conversion of formic acid in the presence of Cu-ZSM-5 samples with identical exchange levels (atomic ratio Cu/Al) prepared using different module zeolites. When the exchange level is ca. 0.42–0.44, the catalytic activity increases non-linearly with an increase in the zeolite module. The Cu-ZSM-5-30 catalysts are most active and Cu-ZSM-5-17 zeolite least active.

Dependences of the catalytic activity and specific catalytic activity of zeolites on the copper content (0.05–2.8 wt%) are shown in Fig. 3. The catalytic activity increases as the copper content up to

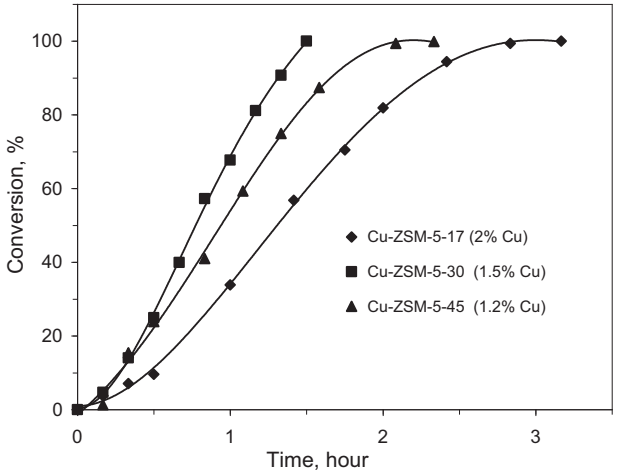

Fig. 2. Formic acid oxidation by hydrogen peroxide over Cu-ZSM-5 zeolites with different Si/Al ratio but similar the exchange level (0.1 M HCOOH, 1 M H_2O_2, 3 g L^{-1} catalyst, initial pH 2.3, 303 K).

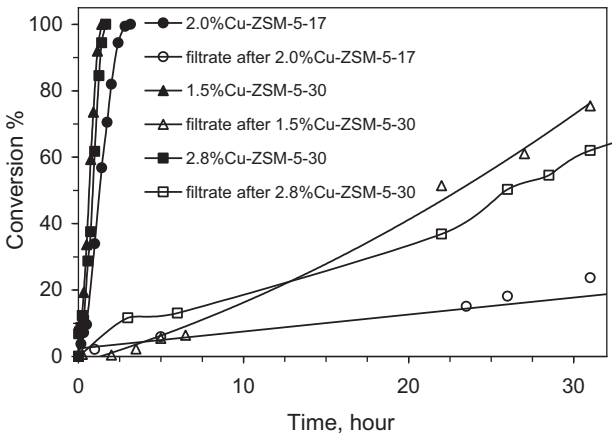

Fig. 4. Test on catalytic activity of the filtrates after the reaction over catalysts Cu-ZSM-5-30 (0.1 M HCOOH, 1 M H_2O_2, 3 g L^{-1} catalyst for experiment over catalyst, initial pH 2.3, 303 K).

0.5 wt%, remains approximately constant at 0.5–1.5 wt% and even decreases slightly at the further increase in the copper content. The specific catalytic activity per gram of Cu decreases with an increase in copper contents. The highest catalytic activity is observed over catalysts based on zeolite with module 30, the lowest with the zeolite with module 17.

Copper concentrations in the solution after the end of the reaction were 0.05–6.5 mg L^{-1} (0.3–10% of the content in the catalyst) for the Cu-ZSM-5-17 catalysts; 0.08–9.0 mg L^{-1} (2.7–14%) for Cu-ZSM-5-30, and 0.8–7.8 mg L^{-1} (4–24%) for Cu-ZSM-5-45. Within each Cu-ZSM-5 series with identical Si/Al ratios, copper was not practically leached from the samples with the exchange level below Cu/Al = 0.2 but leached (from 3 to 10%) at higher levels. Thus, the most stable to copper leaching are Cu-ZSM-5-17 zeolites and the least stable Cu-ZSM-5-45 zeolites. Notice that the copper concentration in the solution not higher than the maximum allowable concentration in drinking water (1 mg L^{-1}) [31] was only observed with the Cu-ZSM-5-17, Cu-ZSM-5-30 and Cu-ZSM-5-45 catalysts containing no more than 1%, 0.5% and 0.3% of copper, respectively. For this reason, the catalysts with low copper contents may only be recommended for practical applications.

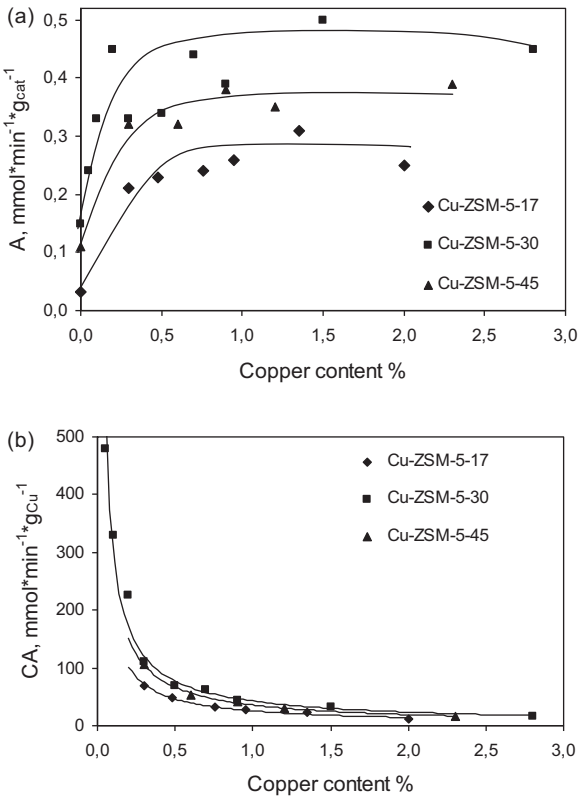

Fig. 3. Influence of the copper content on the catalytic activity (a) and specific catalytic activity (b) of Cu-ZSM-5 with different Si/Al ratio (0.1 M HCOOH, 1 M H_2O_2, 3 g L^{-1} catalyst, initial pH 2.3, 303 K).

The contribution of homogeneous (leached) copper ions to the catalytic activity was studied by testing the activity of the filtered reaction solution. The test reactions with the filtrate were conducted in the presence of 2%Cu-ZSM-5-17, 1.5%Cu-ZSM-5-30, 2.8%Cu-ZSM-5-30 catalysts (Table 2, Nos. 9, 18, and 19) that provided leaching of the maximal absolute quantity of copper (6.5, 6.3 and 9.0 mg L^{-1}, respectively). The reaction rate (Fig. 4) is seen to be lower by three orders of magnitude in the filtrate compared to that in the presence of the heterogeneous catalyst. Hence, it is reasonable to conclude that the activity of Cu-containing zeolites to the peroxide oxidation is accounted for by heterogeneous copper constituent of zeolite but not copper ions leached to the solution.

3.1.4. Oxidation of formic acid in the presence of silicate catalysts Cu-SST

Cu-containing silicate catalysts with the MFI structure and different copper contents (0.5 and 1 wt%) were synthesized by the modified solid state transformation method [28]. XRD studies indicated indeed that the Cu-SST series samples had the MFI structure.

Specific catalytic activities of 0.5% Cu-SST and 1% Cu-SST samples to oxidation of formic acid under identical conditions were 1.6 and 1.9 mmol min^{-1} $g_{Cu}{}^{-1}$, respectively (Table 2, Nos. 26 and 27), i.e. by an order of magnitude lower than the activity of Cu-ZSM-5 zeolites with close copper contents (Table 2, Nos. 5, 7, 12, 14, 19, and 20). The conversion of TOC over Cu-SST was more than 90% in 30 h of the reaction but, nevertheless, not as high as that in the presence of Cu-ZSM-5 catalysts. The reaction solutions were analyzed after the end of the reaction to demonstrate that copper was leached in much larger proportion from Cu-SST (more than 80%) than from ion-exchange Cu-ZSM-5.

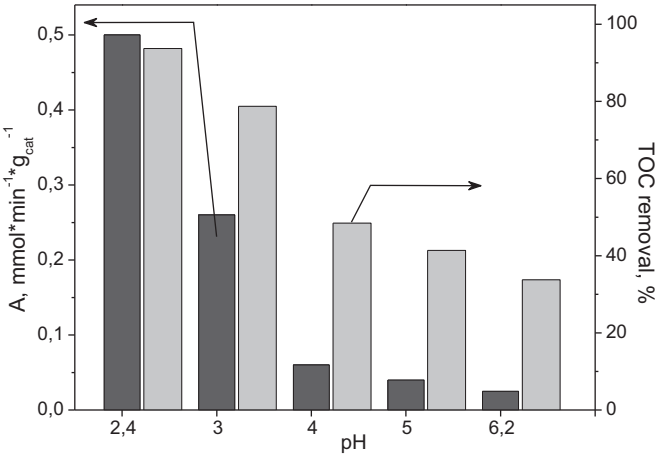

Fig. 5. Influence of the initial pH_0 on the rate of formic acid conversion over zeolite 1.1%Cu-ZSM-5-30 and TOC removal at the end of the reactions (0.1 M HCOOH, 1 M H_2O_2, 3 g L^{-1} catalyst, 303 K).

3.2. The influence of test conditions on the stability and catalytic activity of Cu-ZSM-5 catalysts

In order to choose optimal conditions of the catalyst operation, the influence of temperature, pH, component concentrations on the kinetics and the catalyst stability was studied with 1.1% Cu-ZSM-5-30 as an example. The data obtained are also necessary for understanding the overall reaction mechanism.

3.2.1. The influence of temperature

The influence of temperature was studied at 303, 323 and 343 K. As temperature rose, the oxidation rate increased. Notice that the induction period was not observed in the kinetic curves at 323 and 343 K, probably because the formation of an active form of the catalyst took shorter time than sampling procedure in our experimental technique.

The temperature dependence of the initial rate plotted in the Arrhenius coordinates (Fig. S1) was used for determining the effective activation energy equal to 57.8 ± 1.3 kJ mol^{-1} that is in good agreement with literature data on the apparent activation energy (E_a) for H_2O_2 decomposition over copper complexes supported on silica–alumina supports (50–69 kJ mol^{-1}) [32] and close to the energy observed with CuO/Al_2O_3 (43 kJ mol^{-1}) [33]. Our E_a also is similar to E_a of CWPO of phenol over Cu-containing hydrotacite (56.8 kJ mol^{-1}) [34] and CuO/Al_2O_3 (61.5 kJ mol^{-1}) [33], but higher than that for azo dyes. The latter equals 24.8 kJ mol^{-1} over CuFeZSM-5 [23], 35.9 kJ mol^{-1} over Fe^0 [35], and 25.2 kJ mol^{-1} in the presence of Fe^{2+} [36]. E_a of CWPO over Cu-containing catalysts close to E_a of hydrogen peroxide degradation may indicate that •OH formation by the reaction of H_2O_2 with the catalyst is the rate limiting step.

The catalyst stability to leaching copper ions decreased with temperature elevation. As the temperature was elevated from 303 up to 323 K, copper was leached in a double quantity (31% vs. 14% of the added copper); the leaching reached 38% at 343 K. Hence, it is reasonable to oxidize organic substrates in the presence of copper-containing catalysts at temperatures not higher than 323 K.

3.2.2. Influence of pH of the medium

The maximal catalytic activity of the 1.1%Cu-ZSM-5-30 catalyst was observed in the 0.11 M formic acid solution at initial pH 2.3 (Fig. 5). The catalyst activity decreased considerably upon addition of sodium hydroxide to increase pH. The TOC conversion reached in 2.5 h decreased linearly that correlated to the observed decrease in the catalyst activity and substrate conversion.

The copper concentration in the solution ranges from 0.8 to 1.8 mg L^{-1} that is 1.8 to 4.0% of a total copper introduced with the catalyst into the solution. This is less than the copper quantity leached in the experiments without pH control. This observation agrees with the data obtained earlier [6] with Cu-containing catalysts on oxide supports (SiO_2, Al_2O_3, TiO_2, NaA, NaX) and demonstrates that the copper stability to leaching increases with increasing pH. There may occur two processes in the presence of the Cu-substituted zeolite upon alkalizing the solution by adding sodium hydroxide: (1) substitution of Na^+ for Cu^{2+} in the cation-exchange positions of the zeolite to leach copper and accumulate sodium in the catalyst; (2) hydrolysis of copper cations to form copper oxohydrocomplexes and precipitation of hydroxide-like copper particles (at pH close to 7) to decrease copper leaching and to increase the sodium content. Chemical analysis of the catalyst after the reaction supports these speculations. The copper and sodium contents in the spent catalyst increase with increasing pH from 2.3 to 6.5; they are 0.75 wt% Cu and 1.0 wt% Na at pH 2.4 and 1.35 wt% Cu and 2.9 wt% Na at pH 6.5.

The observed decrease in the catalytic activity with increasing pH may result from a change in the copper state in the catalyst which is, supposedly, indicated by changing colors of the catalyst (from blue to brown) and of the solution (from colorless to brown) after addition of hydrogen peroxide to the catalyst suspension in the formic acid solution at pH 6.5. The change in the copper state also was supported by the UV–vis and ESR data.

To check this hypothesis, experimental studies were carried out by mixing the components (the catalyst, hydrogen peroxide, formic acid, alkali) in different combinations and in different orders. The catalyst color changed to brown, when the alkali was added to the catalyst suspension in 1 M H_2O_2 solution. A decrease in the initial concentration of hydrogen peroxide resulted in the color change at higher pH. For example, the solution became brown colored at pH 8 in 0.5 M hydrogen peroxide and at pH 10 in the 0.18 M solution. These observations led us to conclude that Cu(II) of the catalyst is oxidized to its three-valent state by hydrogen peroxide in an alkali medium than makes it inactive. This process can be described as:

$$2Cu(OH)_{2(solid)} + H_2O_2 + 2OH^- \rightarrow 2CuO_2^- + 4H_2O;$$

where $Cu(OH)_{2(solid)}$ is the active component of catalyst at alkaline pH.

Let us consider how the difference of the equilibrium electrochemical potentials of the process changes on varying pH. The first half-reaction, its standard reduction potential and the Nernst equation [37]:

$$2CuO_2^- + 4H_2O + 2e \rightarrow 2Cu(OH)_{2(solid)} + 4OH^-;$$

$$E_0 = 0.8\,\text{eV}; \qquad E_1 = E_0 + \frac{2.3RT}{2F} \times lg\frac{[CuO_2^-]^2}{[OH^-]^4}$$

The second half-reaction, its standard reduction potential and the Nernst equation for it are [38]:

$$H_2O_2 + 2H^+ + 2e \rightarrow 2H_2O; \qquad E_0 = 1.776;$$

$$E_2 = E_0 + \frac{2.3RT}{2F} \times lg([H_2O_2][H^+]^2).$$

Then the difference of the electrode potentials of the overall reaction is:

$$E_2 - E_1 = 0.976 + 0.03 \times lg\frac{[H_2O_2][H^+]^2[OH^-]^4}{[CuO_2^-]^2}$$

$$= -0.704 + 0.03 \times lg\frac{[H_2O_2]}{[H^+]^2[CuO_2^-]^2}$$

By substituting concentrations $[H_2O_2] = 1$ M, $[CuO_2^-] = 10^{-4}$ M (a total of copper concentration introduced with the catalyst in the solution equals 7×10^{-4} M) at pH 2, we obtain the difference of electrochemical potentials as equal to −0.344 V, i.e. there is no reaction. The difference becomes positive (0.016 V) at pH 8, i.e. the reaction may take place. Thus, increasing pH favors the process of the copper transfer into its inactive state.

Notice that the expression obtained for the electrochemical potential difference is only appropriate for qualitative estimation but not for accurate calculations (there is an unknown equilibrium concentration of CuO_2^- ions and the copper state is different from $Cu(OH)_2$) but can be used for understanding the observed dependence of the catalyst activity on pH and for predicting conditions of the efficient catalyst application. The catalysts can be used either in an acidic medium or at a lower concentration of hydrogen peroxide and, consequently at a lower concentration of the substrate.

3.2.3. Influence of concentrations of formic acid, hydrogen peroxide and the catalyst

The studies were carried out using the 1.1%Cu-ZSM-5-30 by varying one of the parameters at the other parameters maintained constant. The obtained dependences of logarithms of the reaction rates on logarithms of initial concentrations are approximated by straight lines with good correlation coefficients (Fig. S2). The dependence on the initial concentration of the substrate demonstrates that the rate of formic acid oxidation depends only slightly on its initial concentration. At the same time, the influence the hydrogen peroxide concentration and catalyst weight on the rate of the substrate destruction is apparent. The reaction orders were determined as the slope of $\ln W - \ln C$ line to abscissa; they were 0.1 for formic acid, 0.6 for hydrogen peroxide, 0.9 for the catalyst.

The present work was not aimed at the intimate mechanism of CWPO. However, the determined reaction orders allowed us to assume that the limiting stage is activation of hydrogen peroxide on the catalyst surface to form hydroxyl radicals.

3.2.4. Stability of the reused catalysts

Catalysts 1.5%Cu-ZSM-5-30 and 0.5%Cu-ZSM-5-30 were studied in a number of successive cycles of formic acid oxidation in order to characterize the stability of their catalytic properties. In the course of CWPO of organic substrates the catalyst may be deactivated through a loss of the active phase, destruction of the zeolite matrix, blockage of surface centers by the reaction products. Several methods for the regeneration of ZSM-5 catalysts are proposed in literature: calcining in air at 723 K for 10 h [29]; washing with distilled water and drying at 353 K [29], washing with distilled water followed by drying in air at 383 K and calcining at 773 K [4].

In the present work, the catalyst was separated from the reaction mixture after the end of the reaction, washed with distilled water and dried in air at 423 K. The catalyst activities and TOC conversions determined in 2.5 h after beginning of the reaction are shown in Fig. S3. The 1.5%Cu-ZSM-5-30 catalyst activity, as well as TOC conversion is seen not to decrease, within the experimental error, during five cycles of formic acid oxidation. The specific catalytic activity per copper content even increases from 33 to 54 mmol min^{-1} $g_{Cu}{}^{-1}$ that indicates the formation of active component in the course of the reaction. Copper ions are leached in a decreased quantity from cycle to cycle (from 14% in the first cycle to 7.2% in the fifth cycle) to reach a total of 45% of the introduced copper. Copper contents in the solution with the 0.5%Cu-ZSM-5-30 catalyst were ca. 3 times lower. While the catalytic activity remains constant, it is reasonable to suppose that the catalytically inactive copper species are leached. There is practically no cycle-to-cycle change in the silicon (0.02–0.04%) and aluminum (0.2–1.2%) contents in the solution but the quantity of leached iron ions decreases from 18% in the first cycle to 1.5–4% in the second and the following cycles. These are almost the case with the 0.5%Cu-ZSM-5-30 catalyst.

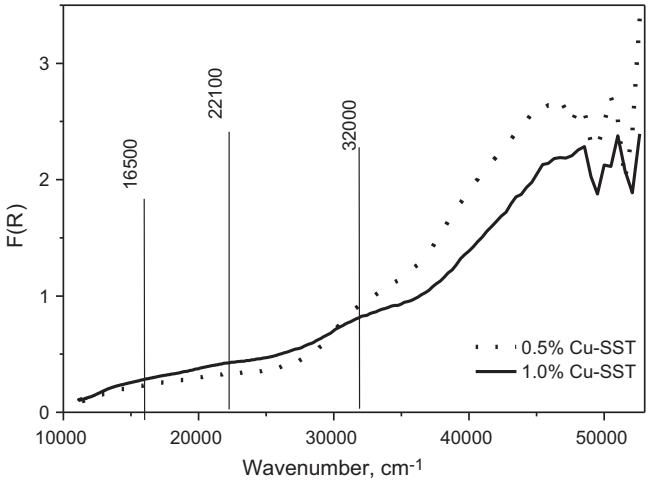

Fig. 6. UV–vis DR spectra of Cu-SST silicates.

XRD technique was used for characterization of the samples used for the first and fifth test cycles. Diffraction patterns of Cu-ZSM-5 acquired before and after cycle 1 show the structure of ZSM-5 with the crystallinity close to 95%, no other phases being formed. After cycle 5, reflections of the zeolite structure (at the 2θ range 22–25°) become less intense but keep their positions. It seems like new nanostructured copper oxide clusters are formed in the zeolite channels.

Emphasize once again that the induction period at the initial segment of the kinetic curve disappear in the second reaction cycle. There may be two reasons: (1) the compounds supported during the catalyst synthesis and blocking the active component are eliminated from the zeolite channels during the first reaction cycle; (2) copper cations are transformed into the active centers in the course of the reaction.

3.3. UV–vis DR and ESR studies of the active metal electron state in the catalyst

3.3.1. UV–vis DR

UV–vis DR and ESR spectroscopic techniques were used for studying the copper electron state responsible for the catalytic activity to CWPO of formic acid.

Cu-SST catalysts are the least active among the copper-containing zeolite catalysts with the MFI structure. Analysis of UV–vis DR spectra (Fig. 6) of the fresh sample revealed that copper cations are involved in square-planar oxide clusters, which are characterized by two absorption bands (a.b.) related to d–d transition (13,300–14,100 cm^{-1}) and a ligand–metal charge transfer band (CTB) (30,000–32,000 cm^{-1}) [26]. Another weak band is observed at 21,800–22,100 cm^{-1}. This band also is observed in UV–vis DR spectra of CuO/Al_2O_3 catalyst and assigned to Cu^+ ions in 3D clusters of CuO [39,40].

The UV–vis DR data obtained with the fresh catalysts agree well with relevant ESR data. In the ESR spectra of Cu-SST recorded both at 77 and at 298 K, there is only a signal with parameters ($g_{||} = 2.38$, $A_{||} = 138$ G, $g_{\perp} = 2.08$) corresponding to isolated copper ions in octahedral oxygen surrounding in fields with tetragonal distortion. However, the intensity ratio in the spectra acquired at 298 and 77 K is much lower (3–5 times) then this must be according to the Curie rule. Such a strong decrease in the signal intensity at 298 K may be accounted for by antiferromagnetic interaction between clustered copper ions. Thus, there are square-planar copper oxide clusters

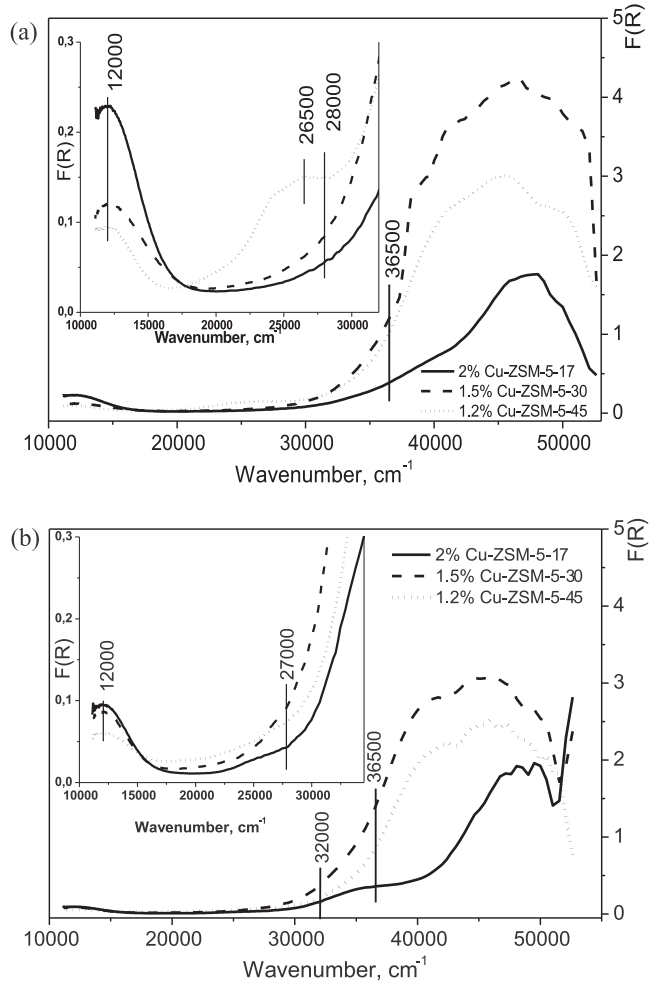

Fig. 7. UV–vis DR spectra of Cu-ZSM-5 catalysts with different Si/Al ratio but similar the exchange level (a) initial; (b) after oxidation of formic acid.

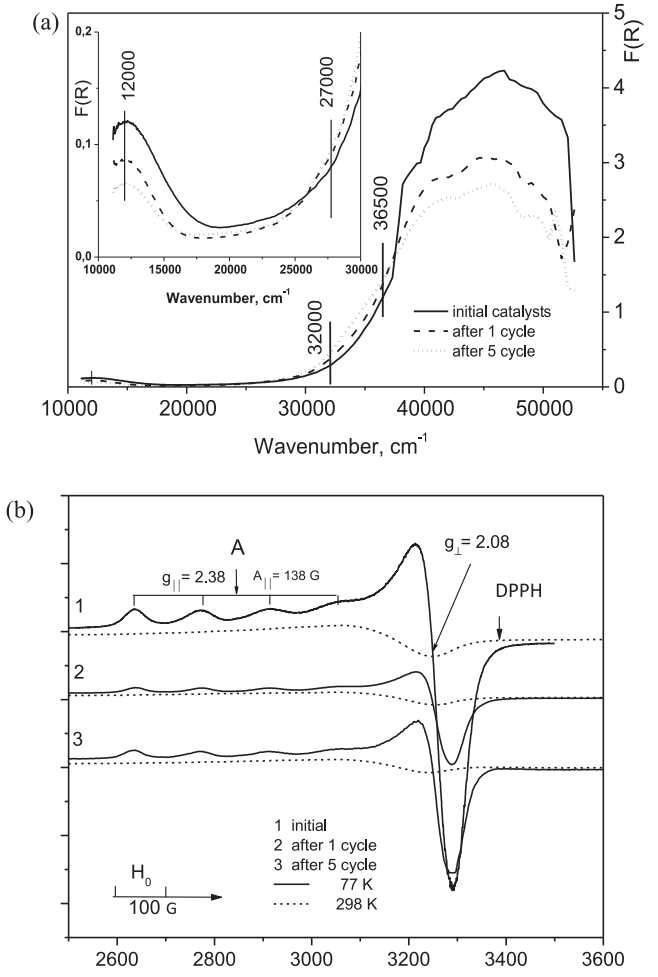

Fig. 8. UV–vis DR (a) and ESR (b) spectra of 1.5%Cu-ZSM-5-30 initial and spent (1 and 5 times).

as precursors of the high-disperse CuO phase in the fresh Cu-SST catalysts; the localization of these clusters (in the channels or on the crystallite surface) is not identified. In the spectra of spent Cu-SST catalysts, both a.b. of d–d transitions (UV–vis) and the signal of isolated copper ions (ESR) are less intense, a strong decrease in the intensity of L–M CTB (30,000–32,000 cm^{-1}) of square-planar copper oxide cluster also being observed.

Fig. 7 shows spectral data acquired with copper-substituted samples 2%Cu-ZSM-5-17, 1.5%Cu-ZSM-5-30, 1.2%Cu-ZSM-5-45 which differ by the zeolite module at a close level of copper substitution. As discussed above, 1.5%Cu-ZSM-5-30 was most active and 2%Cu-ZSM-5-17 least active to oxidation of formic acid by hydrogen peroxide. The following bands are identified in the spectra of the initial samples: (1) an adsorption band at 12,000–12,500 cm^{-1} which is assigned to the d–d transition of isolated Cu^{2+} ions in a weak disordered octahedral coordination of O-containing ligands [26,41], the band intensity being maximal for 2%Cu-ZSM-5-17 and minimal for 1.2%Cu-ZSM-5-45; (2) bands at 27,000–32,000 cm^{-1} which are slightly apparent at the fundamental adsorption edge (FAE) of the zeolite (36,500 cm^{-1}) but characteristic of CTB L → M in copper dimers with one (27,000–28,000 cm^{-1}) and two (32,000 cm^{-1}) oxygen bridge atoms, their intensities, vice versa, being maximal for 1.5%Cu-ZSM-5-30 and minimal for 2%Cu-ZSM-5-17. In addition, there is an absorption band at 26,500 cm^{-1} of 1.2%Cu-ZSM-5-45 (Fig. 7a), which is characteristic of CTB L → M of iron(III) oxide clusters. Such a band is not observed in the spectra of the other sample where Fe^{3+} cations are predominantly in the zeolite lattice.

Inspection of the UV–vis DR and ESR spectra of the spent Cu-ZSM-5 samples, which were tested in CWPO of formic acid at pH 2, leads to conclude about no formation of new electron states of copper but redistribution of copper in different states. In particular, a decrease in the intensity of a.b. 12,000–12,500 cm^{-1} and an increase in the intensity of a.b. 27,000–32,000 cm^{-1} indicates a decrease in the concentration of isolated Cu^{2+} ions (by 45–50%) and an increase in the proportion of square-planar copper oxide/hydroxide clusters in the zeolite channels. In the ESR spectra, there is observed ca. 35–40% decrease in the intensity of the anisotropic signal of the isolated Cu^{2+} ions. The charge transfer band L → M of iron(III) oxide cluster disappears in the spectrum of the spent 1.2%Cu-ZSM-5-45 catalyst (Fig. 7b) that indicates leaching of the iron cations in the course of the reaction. The observed decrease in the intensities of d–d transition and of the ESR signal of isolated copper ions in the spectra is in good agreement with the data of chemical analysis of the spent Cu-ZSM-5 catalysts (Cu/Al > 0.2), which demonstrate that the quantity of copper leached during the reaction increases with an increase in the zeolite module from 17 to 45 and, consequently, with a decrease in the proportion of isolated copper ions in the initial catalyst.

The proportion of square-planar copper oxide clusters increases during the multicycle testing, as well as at the temperature elevation up to 323 and 343 K. Fig. 8 shows a UV–vis DR spectrum acquired with the 1.5%Cu-ZSM-5-30 catalyst after the end

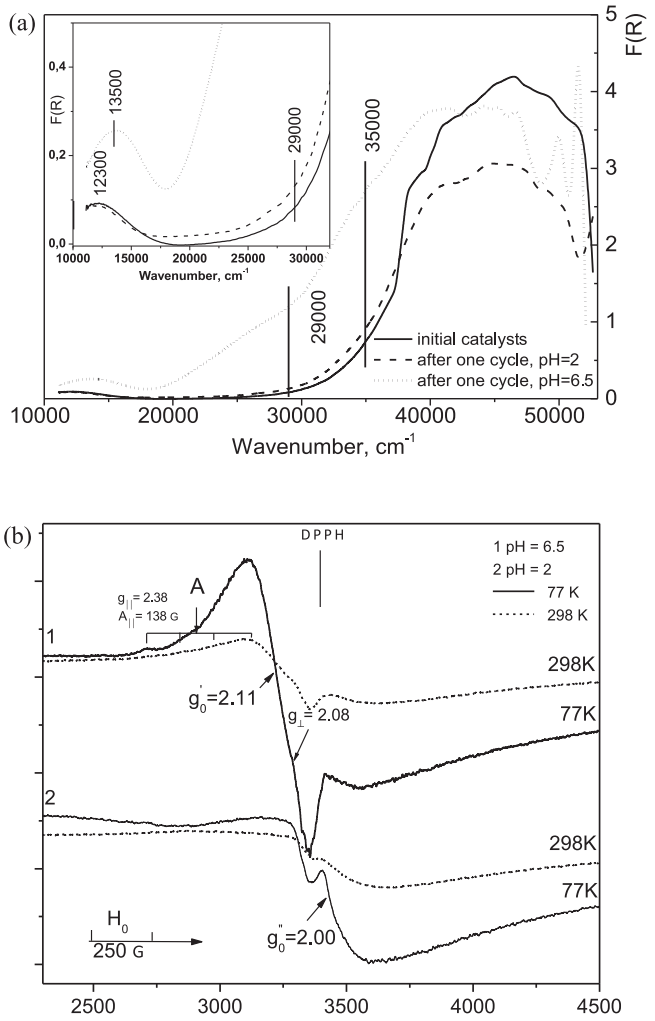

Fig. 9. UV–vis DR (a) and ESR (b) spectra of 1.1%Cu-ZSM-5-30 initial and spent (at initial pH 2 and 6.5) catalysts.

of five cycles of formic acid oxidation. In the spectra of the spent samples, the band of d–d transition of isolated Cu^{2+} ions (12,000 cm^{-1}) decreases gradually in intensity that argues for their decreased concentration, while the intensity of CTB of L → M dimers (27,000 cm^{-1}) and/or square-planar copper clusters (30,000–32,000 cm^{-1}) increases that indicates an increase on the these copper clusters in number. Notice that UV–vis DR and ESR data on 0.5%Cu-ZSM-5-30 argue for a minor decrease in the proportion of the isolated Cu^{2+} ions (no more than 15%) after the fifth test cycle, it being difficult to conclude about accumulation of the square-planar copper clusters due to the low copper concentration in the catalyst and extinction of the L → M charge transfer band. In the spectrum of the sample tested at a higher temperature, e.g. at 323 K, a shoulder at 29,000–32,000 cm^{-1} becomes apparent. In the ESR spectra of the sample tested at 343 K, a symmetrical signal $g_0 = 2.17$ appears at 298 K against a weakly resolute signal of the isolated ions with $g_{II} = 2.32$, $A_{II} = 142$ G and $g_\perp = 2.12$ to indicate the formation of weak magnetic associates of copper ions $Cu^{2+}{}_{Oh}$. The formation of copper ions associates seems to take place owing to their hydrolysis, the rate of hydrolysis increases with elevation of temperature.

It was described in Section 3.2.2 that the activity of the 1.1%Cu-ZSM-5-30 catalyst decreases with increasing pH. The state of copper cations in the catalyst before and after the reaction was characterized using UV–vis DR and ESR spectra (Fig. 9). When pH of the reaction solutions increases due to the addition of NaOH, the concentration of the isolated Cu^{2+} ions with the octahedral oxygen coordination (12,300–12,500 cm^{-1}) in the spent catalysts decreases sharply; the d–d transition of copper ions shifts to 13,500 cm^{-1} due to the strong tetragonal distortion of the oxygen surrounding. The observed band at 13,500 cm^{-1} along with strengthening of the absorption background and appearance of the charge transfer band L → M at 28,000–32,000 cm^{-1} may be an evidence of an increase of the number and growth in size of the square-planar copper oxide or hydrooxo clusters up to the formation of the high-disperse phases of $Cu(OH)_2$ and/or hydrated CuO. Thorough examination of UV–vis DR spectra of the catalysts shows that the intensity of a.b. 20,000–30,000 cm^{-1} is much higher after the reaction at pH 4.5–6.5 then after the reaction at pH 2.4. Absorbance in this region is the superposition of two bands with maxima at 21,500 and 26,500 cm^{-1}. These a.b. are close in energy to CTB L → M of copper peroxocomplexes which were observed with alkaline colloidal solutions of copper hydroxide after adding H_2O_2 [42]. The latter may indicate the formation of stable and therefore inactive copper peroxocomplex.

When the samples were tested at the pH range of 2.4–6.5, pH being controlled by adding NaOH solution, their ESR spectra (77 K) exhibit broad signals with $g_0 = 2.11$ and $g_0 = 2.0$ against a weakly resoluted signal of the isolated ions with $g_{II} = 2.38$, $A_{II} = 138$ G and $g_\perp = 2.08$ (Fig. 9b). The integral intensity of the observed signal of copper ions decreases down to ca. one tenth against that of the initial catalyst. The signal with $g_0 = 2.11$ increases in intensity as pH increases from 2.4 to 6.5 while the signal with $g_0 = 2.00$ decreases. The former signal usually indicate the formation of weak magnetic associates of copper ions, $Cu^{2+}{}_{Oh}$, while strengthening of the exchange interaction between ions results in broadening of the related ESR signal toward its complete disappearance in the spectrum. The broad symmetrical signal with $g_0 = 2.0$ may be assigned to the organic substrate or to the products of its incomplete conversion adsorbed on the catalyst surface, but then this ESR signal should be sufficiently narrower. This signal also may be accounted for by the formation of small α-Fe_2O_3 clusters but this assumption seems hardly probable since the signal intensity is strongly dependent on pH at identical iron concentrations in the spent catalysts. The carbon content is ca. 2 wt% in the sample tested at pH 6.5 that is ca. 15 times higher of that in the catalyst tested at pH 2.3 or at high temperatures. The increased carbon concentration in the spent catalyst leads to conclude about a decrease in the catalyst reactivity with increasing pH. The substrate is adsorbed on the catalyst surface but not oxidized by hydrogen peroxide. Inspection of diffraction patterns acquired with the sample tested at varied pH shows that the lines related to the ZSM-5 channel structure changes more considerably upon an increase in pH to indicate again filling the zeolite channels with oxide clusters.

We can suggest, based on the data obtained, at least two hypotheses to explain the reasons for changes in the copper electron state during the oxidation of formic acid at increasing pH: (1) oxidation of copper in the catalysts to its three-valent state to produce cuprate anion; (2) formation of stable peroxo-species on the surface of copper oxide/hydroxide clusters observed in Refs. [42,43]. However, discrimination of these two hypotheses and these two states of catalyst needs further studies.

The following conclusions are allowed by the analysis of correlations between the catalytic activity of Cu-containing zeolites in the peroxide oxidation of model substrate and electronic state of copper cations in the catalysts before and after the reaction:

1. The maximal activity is provided by dimer or/and square-planar copper oxide clusters, which are stabilized in the zeolite channels of the initial catalyst or formed during the reaction. Supposedly, the clusters located in strictly regular 0.54–0.56 nm

zeolite channels are highly active due to the easy $Cu^{+} \leftrightarrow Cu^{2+}$ transition in the close spaced copper cations and highly stable owing to copper resistance to leaching from the zeolite matrix.
2. Isolated Cu^{2+} cations, when stabilized in the cation exchange positions of the initial catalyst, are much less active than copper oxide clusters but take part in the formation of nanostructured copper oxide clusters during the reaction. This is most likely to cause the shortage and disappearance of the induction period in the kinetic curves.
3. The formation of large copper oxide clusters on the crystallite surface is characteristic of the catalysts prepared by the method of solid phase transformation. The clusters are soluble in the substrate solution that results in copper leaching and in the low activity of the catalyst.

4. Conclusions

Catalytic properties of Cu- and Fe-substituted zeolites with the MFI morphology in wet peroxide oxidation of formic acid as a model organic substrate were thoroughly studied. The studies were focused on the influence of the method for introduction of the transition metal ion into the zeolite matrix (ion exchange and solid phase synthesis), transition metal cation nature (Cu, Fe) and content (0–2.8 wt%) on the electron state of the transition metal and on catalytic properties of zeolites.

Cu-substituted ZSM-5 zeolites with the atomic ratio Si/Al = 30 and Cu content of 0.5–1.5, which are prepared by ion exchange are shown to be most promising for CWPO. Destruction of formic acid over these catalysts reaches 99% in 1.5 and 0.5 h at 303 and 323 K, respectively, the proportion of leached copper from the catalyst being not higher than 15%. As a result, there is no decrease in the catalyst activity during at least 5 cycles of the reaction. In the case of Fe-ZSM-5 zeolite with 0.5–0.6 wt% Fe introduced by the template synthesis, similar destruction level is reached in 3–4.5 h.

Kinetic studies of the reaction depending on the reaction conditions allowed the reaction orders in respect of concentrations of the substrate, oxidant and catalyst, the activation energy and optimal pH of the medium to be determined. The data obtained will be further used for choosing optimal conditions and for mathematical modeling of the processes of water treatment.

Electron states of copper and iron ions were studied in the fresh and spent catalysts. It was supposed that the high efficiency of Cu-ZSM-5 in redox reactions in aqueous media is provided by copper–oxygen dimers and nanostructured square-planar copper oxide clusters localized in the zeolite channels. These structures are formed not only in the course of the catalyst preparation but also from closely spaced isolated Cu^{2+} ions in the zeolite channels during the oxidation reaction. The formation of nanostructured copper clusters in regular 0.54–0.56 nm zeolite channels provides the high stability to copper leaching from the zeolite matrix in aqueous media and the high activity to redox reactions owing to the easy $Cu^{+} \leftrightarrow Cu^{2+}$ transition in the close spaced copper cations. In the copper-containing catalysts prepared by solid state transformation, large copper oxide clusters are formed on the zeolite crystallite surface to cause low catalyst activity and copper leaching in acidic solutions formed upon destruction of organic compounds.

Acknowledgements

We thank Dr. Ushakov V.A. for the XRD analysis and Vasenin N.T. for ESR experiments. This work was partially financially supported by the Russian Fund of Basic Research and Ukrainian National Academy of Science (grants 08-03-90435 and 12-03-90404) and Russian Federation President Grant for the Leading Scientific Schools N NSh-524.2012.3. Their supports are gratefully acknowledged.

Appendix A. Supplementary data

Supplementary data associated with this article can be found, in the online version, at http://dx.doi.org/10.1016/j.apcatb.2013.04.050.

References

[1] S. Vilhunen, M. Sillanpaa, Reviews in Environmental Science and Biotechnology 9 (2010) 323–330.
[2] M. Neamtu, C. Zaharia, C. Catrinescu, A. Yediler, M. Macoveanu, A. Kettrup, Applied Catalysis B: Environmental 48 (2004) 287–294.
[3] J. Prousek, Chemicke Listy 89 (1995) 11–21.
[4] G. Centi, S. Perathoner, T. Torre, M.G. Verduna, Catalysis Today 55 (2000) 61–69.
[5] A. Sychev, V. Isac, Russian Chemical Reviews 64 (1995) 1105–1129.
[6] O. Pestunova, G. Elizarova, Z. Ismagilov, M. Kerzhentsev, V. Parmon, Catalysis Today 75 (2002) 219–225.
[7] R. Liou, S. Chen, Journal of Hazardous Materials 172 (2009) 498–506.
[8] J. Botas, J. Melero, F. Martinez, M. Pariente, Catalysis Today 149 (2010) 334–340.
[9] S. Caudo, G. Centi, G. Genovese, S. Perathoner, Applied Catalysis B: Environmental 70 (2007) 437–446.
[10] J. Barrault, M. Abdellaoui, C. Bouchoule, A. Majeste, J.M. Tatibouet, A. Louloudi, N. Papayannakos, N. Gangas, Applied Catalysis B: Environmental 27 (2000) 225–230.
[11] S. Kim, D. Lee, Catalysis Today 97 (2004) 153–158.
[12] J. Sotelo, G. Ovejero, F. Martinez, J. Melero, A. Milieni, Applied Catalysis B: Environmental 47 (2004) 281–294.
[13] I. Castro, F. Stuber, A. Fabregat, J. Font, A. Fortuny, C. Bengoa, Journal of Hazardous Materials 163 (2009) 809–815.
[14] G. Ovejero, J. Sotelo, F. Martinez, J. Melero, L. Gordo, Industrial and Engineering Chemistry Research 40 (2001) 3921–3928.
[15] D. Doocey, P. Sharratt, Process Safety and Environmental Protection 82 (2004) 352–358.
[16] A. Kondru, P. Kumar, S. Chand, Journal of Hazardous Materials 166 (2009) 342–347.
[17] M. Dukkanci, G. Gunduz, S. Yilmaz, Y. Yaman, R. Prikhod'ko, I. Stolyarova, Applied Catalysis B: Environmental 95 (2010) 270–278.
[18] I. Stolyarova, I. Kovban', R. Prikhod'ko, A. Kushko, M. Sychev, V. Goncharuk, Russian Journal of Applied Chemistry 80 (2007) 746–754.
[19] E. Parkhomchuk, M. Vanina, S. Preis, Catalysis Communications 9 (2008) 381–385.
[20] S. Valange, Z. Gabelica, M. Abdellaoui, J. Clacens, J. Barrault, Microporous and Mesoporous Materials 30 (1999) 177–185.
[21] K. Valkaj, A. Katovic, S. Zrncevic, Journal of Hazardous Materials 144 (2007) 663–667.
[22] K. Pirkanniami, M. Sillanpaa, Chemosphere 48 (2002) 1047–1060.
[23] M. Dukkanci, G. Gunduz, S. Ylmaz, R. Prihod'ko, Journal of Hazardous Materials 181 (2010) 343–350.
[24] S. Perathoner, G. Genti, Topics in Catalysis 33 (2005) 207.
[25] O. Taran, E. Polyanskaya, O. Ogorodnikova, V. Kuznetsov, V. Parmon, M. Besson, C. Descorme, Applied Catalysis A: General 387 (2010) 55–66.
[26] S. Yashnik, Z. Ismagilov, V. Anufrienko, Catalysis Today 110 (2005) 310–322.
[27] P. Ratnasamy, R. Kumar, Catalysis Today 9 (1991) 329.
[28] E. Sendel, Colorimetric Determination of Traces of Metals, Interscience Publishers, Inc., New York, 1959.
[29] K. Fajerwerg, Applied Catalysis B: Environmental 10 (1996) 229.
[30] E. Kuznetsova, E. Savinov, L. Vostrikova, V. Parmon, Applied Catalysis B: Environmental 51 (2004) 165.
[31] Collection of Sanitary Standards and Methods of Control of Harmful Substances in the Environment, Art, Moscow, 1991, pp. 370 (in Russian).
[32] I. Salem, M. Salem, A. Gemeay, Journal of Molecular Catalysis 84 (1993) 67–75.
[33] N.S. Inchaurrondo, P. Massa, R. Fenoglio, J. Font, P. Haure, Chemical Engineering Journal 198/199 (2012) 426–434.
[34] S. Zhou, Z. Qian, T. Sun, J. Xu, C. Xia, Applied Clay Science 53 (2011) 627–633.
[35] J. Fan, Y. Guo, J. Wang, M. Fan, Journal of Hazardous Materials 166 (2009) 904–910.
[36] H. Xu, D. Zhang, W. Xu, Journal of Hazardous Materials 158 (2008) 445–453.
[37] Z. Galus, J. Hoare, in: A.I. Bard, R. Parsons, J. Jordan (Eds.), Standard Potentials in Aqueous Solutions, Marcel Dekker, New York, 1985, pp. 57–198.
[38] K.A. Khokryakov, S.A. Simanova, in: S.A. Simanova (Ed.), New Handbook of Chemist and Technologist. Electrode Processes. Chemical Kinetics and Diffusion. Colloid Chemistry, Professional, St. Petersburg, 2004, p. 16 (in Russian).
[39] G. Centi, S. Perathoner, D. Biglino, E. Giambello, Journal of Catalysis 152 (1995) 75–92.
[40] M. Marion, E. Garboeski, M. Primet, Journal of the Chemical Society, Faraday Transactions 86 (1990) 3027–3032.
[41] F. Hadzhieva, V. Anufrienko, T. Yurieva, V. Vorobiev, T. Minyukova, Reaction Kinetics and Catalysis Letters 30 (1986) 85–92.
[42] G.L. Elizarova, G.V. Odegova, L.G. Matvienko, E.P. Talsi, V.N. Kolomiychuk, V.N. Parmon, Kinetics and Catalysis 44 (2) (2003) 210–222.
[43] S. Caudo, G. Centi, C. Genovese, S. Perathoner, Topics in Catalysis 40 (2006) 207–219.